

Broadband Purcell enhanced emission dynamics of quantum dots in linear photonic crystal waveguides

A Laucht^{1,2}, T Günthner^{1,3}, S Pütz¹, R Saive¹, S Frédérick^{1,4},
N Hauke¹, M Bichler¹, M-C Amann¹, A W Holleitner¹,
M Kaniber¹, and J J Finley¹

¹ Walter Schottky Institut and Physik-Department, Technische Universität München, Am Coulombwall 4a, 85748 Garching, Germany

²Centre for Quantum Computation & Communication Technology, The University of New South Wales, Sydney NSW 2052, Australia

³Institut für Experimentalphysik, Universität Innsbruck, Technikerstrasse 25, 6020 Innsbruck, Austria

⁴National Research Council of Canada, Ottawa, ON, Canada

E-mail: finley@wsi.tum.de

Abstract. The authors investigate the spontaneous emission dynamics of self-assembled InGaAs quantum dots embedded in GaAs photonic crystal waveguides. For an ensemble of dots coupled to guided modes in the waveguide we report spatially, spectrally, and time-resolved photoluminescence measurements, detecting normal to the plane of the photonic crystal. For quantum dots emitting in resonance with the waveguide mode, a $\sim 21\times$ enhancement of photoluminescence intensity is observed as compared to dots in the unprocessed region of the wafer. This enhancement can be traced back to the Purcell enhanced emission of quantum dots into leaky and guided modes of the waveguide with moderate Purcell factors up to $\sim 4\times$. Emission into guided modes is shown to be efficiently scattered out of the waveguide within a few microns, contributing to the out-of-plane emission and allowing the use of photonic crystal waveguides as broadband, efficiency-enhancing structures for surface-emitting diodes or single photon sources.

PACS numbers: 42.50.Ct, 42.70.Qs, 78.67.Hc, 78.47.-p, 42.82.Et

Photonic crystal waveguides (PCWs) are of strong interest as optical elements for integrated nanophotonic optical circuits and on-chip quantum optics applications. [1, 2, 3, 4, 5] They have been used to route single photons from cavity-coupled [2, 6, 7, 5] and waveguide-coupled quantum dots (QDs) [8, 9], but also to tailor the local density of optical states (LDOS) an emitter experiences. This method to modify the LDOS experienced by an emitter provides a route to engineer the rate and directionality of spontaneous emission. [10, 11, 12, 13, 14, 15, 16, 17, 18, 19, 20, 21, 5, 22] This is a key concept to enhance the efficiency of nanoscale light sources such as single photon sources [23, 24, 25, 26, 27, 28] and nanoscale lasers. [29] Recently, Kaniber et al. [30] demonstrated a $\sim 16\times$ enhanced extraction efficiency for single QDs emitting into the two-dimensional photonic bandgap of a photonic crystal. The photonic bandgap inhibits photon emission into the in-plane direction and redistributes it into out-of-plane modes, effectively increasing the extraction efficiency. However, this comes at the cost of long radiative lifetimes, imposing an inherent jitter in the photon emission time, a source of quantum distinguishability. [31, 32] In contrast, strong enhancements of spontaneous emission rates have been observed for QDs in low mode volume, high-Q cavities. [33, 34, 7] However, these systems require a sophisticated electro- [35] or thermo-optical [36] tuning method to spectrally bring the emitter and cavity mode into resonance.

In this paper we demonstrate the advantage of using a PCW mode to enhance the emission rate and the extraction efficiency of an ensemble of QDs over a wide spectral range of ~ 18 meV in the out-of-plane direction. We compare the emission properties normal to the sample surface for QDs in the bulk GaAs, the photonic crystal membrane (PC) and the PCW region. Measurements were made for QDs in and out of spectral resonance with the guided PCW mode. These measurements show a strong enhancement of the photoluminescence (PL) intensity up to $\sim 21\times$ for QDs spatially and spectrally coupled to the waveguide mode compared to QDs in the unprocessed bulk material. We attribute this enhancement to a combination of angular redistribution of emission into leaky PCW modes and Purcell enhanced emission into the guided PCW mode with subsequent scattering into leaky modes.

The sample investigated was grown by molecular beam epitaxy and consists of a 500 nm thick $\text{Al}_{0.8}\text{Ga}_{0.2}\text{As}$ sacrificial layer, and a 180 nm thick undoped GaAs layer with a single layer of nominally $\text{In}_{0.5}\text{Ga}_{0.5}\text{As}$ QDs at its midpoint. The sample has a dot density of $\rho_{QD} > 50 \mu\text{m}^{-2}$. A two-dimensional PC formed by defining a triangular array of air holes was realized using a combination of electron-beam lithography and reactive ion etching. PCWs were established by introducing line defects consisting of a single missing row of holes (W1 waveguide). Free standing GaAs membranes were created in a final wet etching step using hydrofluoric acid.

For optical characterization the sample was mounted in a liquid He-flow cryostat and cooled to 10 – 15 K. For excitation we used a pulsed Ti-Sapphire laser (80 MHz repetition frequency, 6 ps pulse duration) tuned to the low energy absorption edge of the bulk GaAs ($\lambda_{laser} = 815$ nm). Excitation of the QDs and detection of the emitted PL

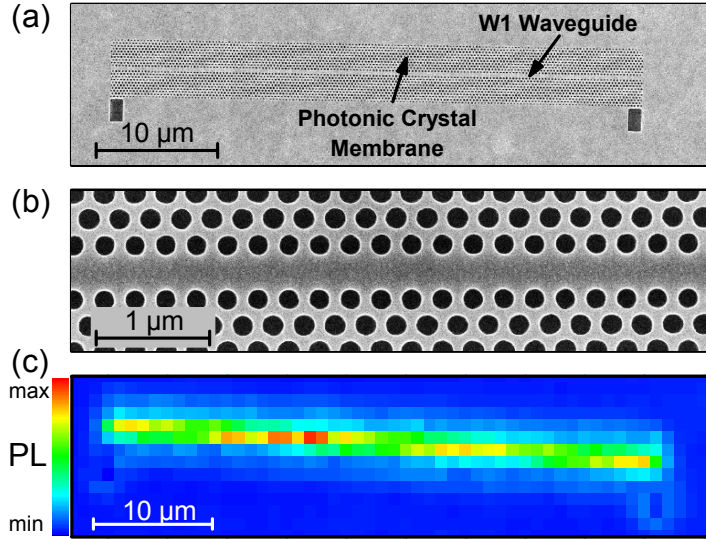


Figure 1. (a) and (b) Scanning electron microscope images of the investigated W1 waveguide - quantum dot system from the top. (c) Spatially-resolved scan of the photoluminescence signal performed with excitation and detection from the top and integrated over the 1298 - 1340 meV spectral range. The area of high photoluminescence intensity corresponds to the waveguide region.

signal was done perpendicular to the sample surface using a 100× microscope objective (NA=0.50). The full-width-half-maximum ($FWHM$) of the excitation laser spot on the sample was determined to be $FWHM \sim 1.3 \mu\text{m}$, while the size of the detection spot had a diameter of $FWHM \sim 6.0 \mu\text{m}$. The QD PL was spectrally analyzed using a 0.5 m imaging monochromator and detected using a Si-based, liquid nitrogen cooled CCD detector. For time-resolved spectroscopy we used a Si-based avalanche photodiode connected to the side-exit of our monochromator providing a temporal resolution of ~ 350 ps.

In Fig. 1(a) and (b) we present a scanning electron microscope image of a nominally identical sample to the one used for the PL measurements. The photonic structure has a total length of $45 \mu\text{m}$, a slab thickness of $h = 180$ nm, a PC lattice constant of $a = 270$ nm, and an air hole radius to lattice constant ratio of $r/a = 0.34$. The two rectangles directly next to the photonic crystal structure serve for orientation purposes during optical measurements and have no influence on the photonic properties of the waveguide. We obtained a spatially and spectrally resolved PL map of this particular structure by scanning the laser spot over the surface of the sample and recording a PL spectrum at every position in a confocal detection geometry. A typical result of this scan is presented in Fig. 1(c) where we have integrated the detected PL over the spectral range of the QDs (1298 meV to 1340 meV) and plotted the resulting intensity in a false color representation. The contours of the photonic structure can be easily recognized in the PL map and we observe a clear luminescence enhancement on the photonic structure compared to the unpatterned substrate.

We now investigate the origin of this PL enhancement. To do this, we performed photonic bandstructure calculations using the software package RSoft. [37] We use the appropriate parameters for GaAs of $n_{\text{GaAs}} = 3.5$ and the geometric parameters of $h/a = 0.6667$ and $r/a = 0.34$, corresponding to the investigated W1 PCW. The result of this simulation is plotted in Fig. 2(a) where we plot the normalized frequency of the photonic bands as a function of k-vector on the path from the Γ point to the K' point. [38, 39] We present the PCW modes as blue solid lines, the slab waveguide modes as light gray regions, and the lossy region above the light cone is shaded in dark gray. The region above the light cone corresponds to the energy-wavevector combinations for which photons are not confined to the slab by total internal reflection, i.e. they can leave the waveguide in vertical directions. We calculate the guided part of the lowest energy waveguide (0th order) mode WM1 to be at a normalized frequency of $a/\lambda = 0.262 - 0.274$ which corresponds to an energy of $E = 1203 - 1259$ meV. For small wavevectors $k < 0.28$ this mode overlaps with the region above the light cone. Photons of these wavevector-energy combinations can, therefore, couple to free space modes and leave the sample in vertical directions. This unguided part of the waveguide mode spans the normalized frequency range of $a/\lambda = 0.275 - 0.308$ ($E = 1260 - 1413$ meV). The second waveguide (1st order) mode WM2 extends from $a/\lambda = 0.285 - 0.296$ ($E = 1309 - 1359$ meV) with an additional unguided region at $a/\lambda = 0.291 - 0.296$ ($E = 1338 - 1359$ meV). The third waveguide (second order) mode WM3 is at much higher energies of $a/\lambda = 0.334 - 0.337$ ($E = 1534 - 1548$ meV) (data not shown).

For comparison we plot two examples of PL spectra in Fig. 2(b). The blue line corresponds to a spectrum recorded directly on the PCW, while the black line corresponds to a spectrum recorded next to the PCW on the unprocessed GaAs bulk material (note the $\times 5$ magnified scale). We clearly observe a strong enhancement of the PL intensity in the spectral range between 1300 meV and 1325 meV. For these excitation conditions, we detect the maximum signal of ~ 78000 cts/s at an energy of ~ 1317 meV, $\sim 21\times$ stronger than the ~ 3700 cts/s obtained from the unprocessed bulk material. The intensity oscillations in the spectrum recorded on the PCW structure, most likely originate from Fabry-Perot resonances due to the finite length of the waveguide. [22] We notice that the energy range over which we observe PL enhancement coincides very well with the flat part of the dispersion relation of the second energy mode, but also with the energy range of the unguided parts of the first and the second waveguide mode as shown in Fig. 2(a).

We continue investigating this system by performing time-resolved measurements on the W1 waveguide for 200 different energies in the range between 1239.8 meV and 1377.6 meV. To do this we used the spectrometer as a spectral bandpass filter of width ~ 0.25 meV and recorded multiple decay transients as a function of energy. The measured data was then fitted with an automated fitting algorithm, taking into account the instrument response function of the experimental setup. The algorithm first tries to fit a bi-exponential decay but automatically switches to a mono-exponential decay when one of the fitting parameters is regarded unrealistic. This is the case when (i) one of the

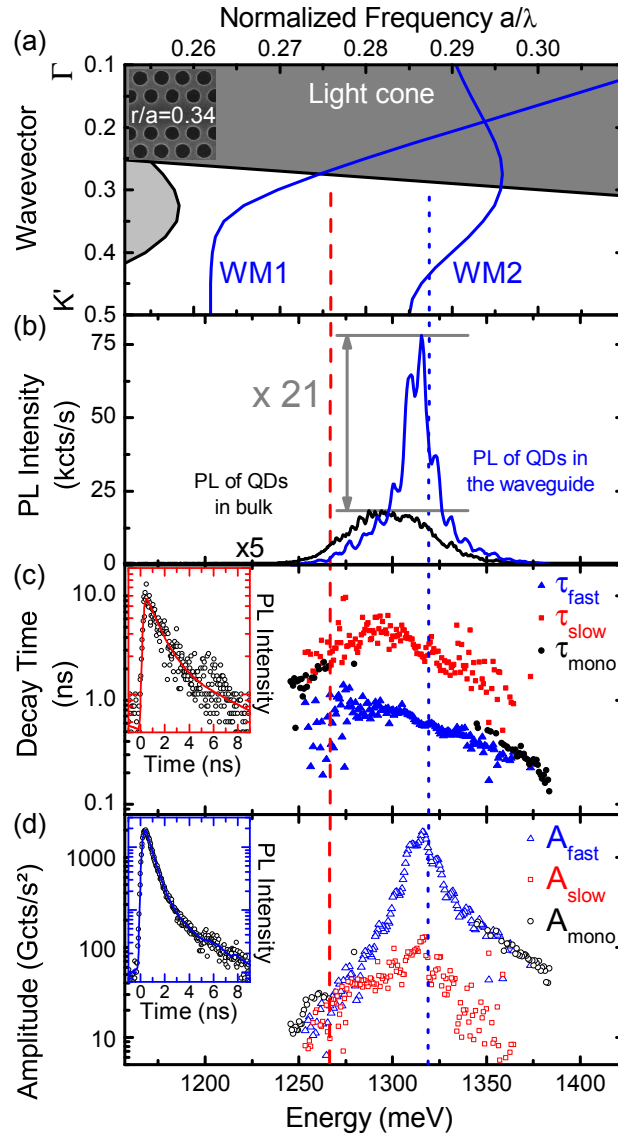


Figure 2. (a) Photonic bandstructure calculations for a W1 waveguide with $r/a = 0.34$ and $h/a = 0.6667$. The blue lines correspond to the photonic waveguide modes and the light gray region to the slab waveguide modes. The dark gray region indicates the region above the light cone. (inset) Scanning electron microscope image of the investigated photonic crystal waveguide structure. (b) Comparison of the photoluminescence signal measured on the ensemble of quantum dots in the unprocessed bulk material (black line) and on the ensemble of quantum dots in the waveguide region (blue line). (c) and (d) Fitting parameters of the decay transients measured on the photonic crystal waveguide as a function of energy. In (c) the extracted decay times and in (d) the corresponding amplitudes are plotted. The black circles correspond to the decay parameters obtained from mono-exponential fits, while the blue triangles (red squares) correspond to the fast (slow) component of the bi-exponentially fitted decay transients. (insets) Decay transients and fits at the energy of 1275 meV (indicated by the red dashed line) for the upper, red-framed inset and 1318 meV (indicated by the blue dotted line) for the lower, blue-framed inset.

amplitudes becomes negative, (ii) the two lifetimes differ by less than 20%, (iii) one of the lifetimes is shorter than 50 ps, or (iv) one of the amplitudes is more than $25\times$ larger than the other one. In Fig. 2(c) the extracted decay times are shown and in Fig. 2(d) the corresponding amplitudes are plotted. The blue triangles (red squares) correspond to the fast (slow) component of the bi-exponentially fitted decay parameters. When a decay is fitted mono-exponentially the resulting parameters are plotted as black circles.

The decay dynamics can predominantly be fitted with bi-exponential parameters close to the resonance with the maximum PL enhancement at ~ 1317 meV, and with mono-exponential parameters off resonance. We interpret this observation according to the fact that only the emission dynamics of QDs spatially located in the waveguide region and spectrally in resonance with the PCW mode can be enhanced by the Purcell effect. However, our experiment detects contributions of spatially coupled *and* uncoupled QDs since our excitation spot size is $4 - 5\times$ larger than the PCW width. In resonance with the PCW mode the decay times typically exhibit values of $\tau_{fast} = 0.57 \pm 0.1$ ns and $\tau_{slow} = 2.7 \pm 0.1$ ns. The Purcell enhanced decay times are longer than the ones that have been observed for QDs coupled to a photonic crystal cavity mode. [33, 40, 34, 41] We attribute this to the combined influence of an averaging effect over QDs that are spatially well and badly coupled to the PCW mode, the slope of the second PCW mode in k-space which leads to a lower photonic density of states, and additional broadening of the mode due to fabrication imperfections.[13] We also notice a general energy dependence of the decay times. At lower energies we observe longer decay times than at higher energies. We relate this to the enhanced contribution of fast multi-excitonic states to the PL signal at higher energies. [42, 43] The amplitude of the fast decay component, plotted in Fig. 2(d), nicely resembles the profile of the enhanced PL spectrum in Fig. 2(b), while the amplitude of the slow decay component stays almost constant (note the logarithmic scale).

We present two decay transients with fits as examples in the insets of Fig. 2 (c) and (d). The decay transient in Fig. 2(c) - inset was recorded off resonance at the energy of 1275 meV (indicated by the red dashed line), and the transient in Fig. 2(d) - inset in resonance at the energy of 1318 meV (indicated by the blue dotted line). Both transients exhibit a bi-exponential decay, albeit with a larger amplitude and shorter decay time of the fast decay component of the resonant transient. This is in good agreement with the extracted parameters presented in Fig.2 (c) and (d).

At first sight, the observation of a larger emission amplitude in the direction normal to the photonic crystal membrane may seem counter-intuitive. In ideal structures we would expect the Purcell enhanced emission to be efficiently guided away from the excitation spot along the waveguide, resulting in a decrease of emission detected in the vertical direction. However, disorder is known to lead to a scattering of the guided light via Anderson localization and radiation normal to the surface of the waveguide. [44, 45, 20] Indeed, recent near field measurements of the frequency dependence of the PCW mode in similar systems have revealed direct evidence for localization and its increasing importance for slow light modes. [46] Scattering in the

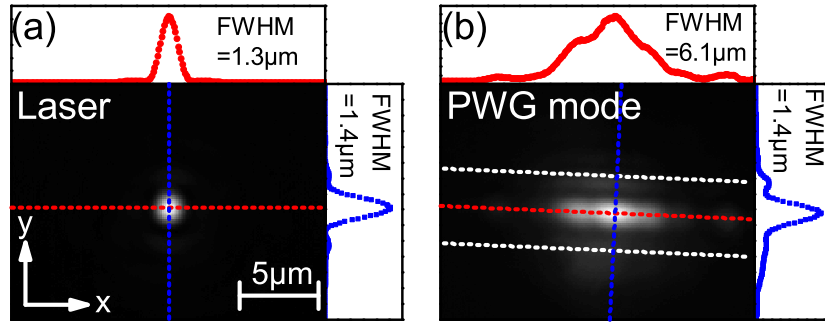


Figure 3. (a) Spatial image of the reflection of the laser spot on the sample surface. (b) Spatial image of the photoluminescence signal of the waveguide mode normal to the sample surface (filtered with a 10nm bandpass filter at the energy of the mode). The dotted white lines indicate the outline of the photonic crystal membrane.

in-plane direction is inhibited due to the photonic bandgap of the surrounding photonic crystal, but scattering into modes above the light cone that can readily escape from the slab is still possible. [47, 48, 49] Furthermore, the finite length of the PCW structure also enables the QDs to emit in vertical directions due to Fabry-Perot effects. [50] In our structures, probably the most important reason for emission in vertical directions is the presence of non-guided waveguide modes with the same energy that can be accessed by scattering induced by disorder. QDs can emit light directly into the leaky modes, or propagating photons from the guided mode can be scattered into these modes due to disorder in the crystal. [47, 15, 48, 49, 22] Similar experimental observations have been made by Stumpf et al. [15], and recently by Hoang et al. [22] and Huisman et al. [46]

In order to support these suggestions we performed additional measurements with a Si-based, Peltier-cooled CCD camera for spatial imaging. In Fig. 3(a) we present an image taken of the laser excitation spot on the sample surface at an energy of 1521 meV. The red (blue) curve corresponds to the cross section along the x- (y-) direction at the position indicated by the red (blue) line. From these plots, we can extract the $FWHM$ of the laser spot to be $\sim 1.3 \mu\text{m}$ in both the x- and the y-directions. Fig. 3(b) shows a similar image of the PL emitted by the PCW mode in the vertical direction. In order to record this image, we mounted a 10 nm-bandpass filter, centered at the energy of the strongest PL enhancement, in front of the camera. While the PL signal recorded along the y-axis, perpendicular to the waveguide direction, exhibits a similar width as the reflection of the laser spot $FWHM = 1.4 \mu\text{m}$, the signal along the waveguide direction (x-axis) is much broader with $FWHM = 6.1 \mu\text{m}$. This observation strongly supports the assertion, that light efficiently emitted into the nominally guided waveguide mode is scattered into vertical directions due to the processes mentioned above. Since our detection spot has a size of $FWHM \sim 6.0 \mu\text{m}$, we collect most of this scattered light and observe, therefore, not only PL emitted into the vertical direction, but also PL emitted into the guided modes and subsequently scattered into the vertical direction.

We check for Purcell-enhanced emission by performing a spatially-resolved scan

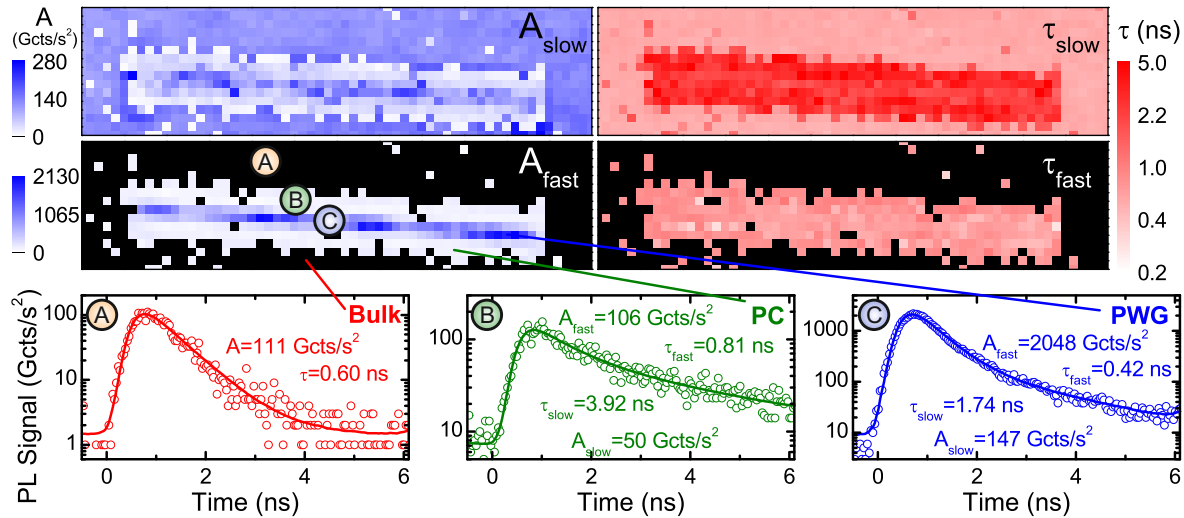


Figure 4. Spatially-resolved scan of the time-resolved photoluminescence signal. The different panels show the fitted amplitude A_{slow} and decay time τ_{slow} of the slow decay component and the amplitude A_{fast} and decay time τ_{fast} of the fast decay component. **A**, **B** and **C** present examples of decay transients of the spatially-resolved scan recorded at the position **A** the bulk material, **B** the photonic crystal membrane, and **C** the photonic crystal waveguide.

of the time-resolved PL signal emitted at the peak of the amplitude (1317 meV). In order to do this we scan the excitation spot over the surface of the sample in $1 \mu\text{m}$ -steps and record the decay transients at every position over a 61×16 matrix. The decay transients are then fitted taking into account the instrument response function of the experimental setup. The same fitting algorithm as before was used, which first tries to fit a bi-exponential decay but automatically switches to a mono-exponential decay when one of the fitting parameters becomes unrealistic. The result of the fitting routine is summarized in the different panels of Fig. 4 that show the amplitude A_{slow} and decay time τ_{slow} of the slow decay component and A_{fast} and τ_{fast} of the fast decay component. When the decay transient is fitted mono-exponentially, the extracted amplitude and decay time are plotted in the panels for the slow decay component and the corresponding pixel in the panels for the fast decay component are blackened.

We can clearly recognize the outline of the PCW structure from the data in Fig. 4. On the unprocessed bulk material the decay transients are globally well described by mono-exponential decays, leading to the large blackened area around the photonic crystal membrane structure (see e.g. position **A** on Fig. 4). We present a typical example of one of these decay transients in the panel of Fig. 4, marked by **A**. The amplitude and the decay time of the mono-exponential decay are fitted to be $A_{bulk} = 111 \pm 14 \text{ Gcts/s}^2$ and $\tau_{bulk} = 0.6 \pm 0.1 \text{ ns}$, which results in an intensity of $I_{bulk} = A_{bulk} \cdot \tau_{bulk} = 67 \pm 14 \text{ cts/s}$. The extracted parameters of the decays at the different positions are summarized in Tab. 1.

Upon moving away from the bulk material onto the photonic crystal membrane,

Position	τ (ns)	A (Gcts/s ²)	I (cts/s)	I_{total} (cts/s)
Ⓐ Bulk	0.60 ± 0.1	111 ± 14	67 ± 14	67 ± 14
Ⓑ Photonic Crystal Membrane	0.81 ± 0.1	106 ± 12	86 ± 14	282 ± 32
	3.92 ± 0.1	40 ± 4	196 ± 18	
Ⓒ Photonic Crystal Waveguide	0.42 ± 0.1	2048 ± 87	860 ± 208	1116 ± 234
	1.74 ± 0.16	147 ± 7	256 ± 26	

Table 1. Overview on the extracted decay times and amplitudes for Ⓐ the bulk material, Ⓑ the photonic crystal membrane, and Ⓒ the photonic crystal waveguide.

but not on the W1 waveguide, the decay transients become clearly bi-exponential. A representative transient is presented in Fig. 4 and marked by Ⓑ. Here, we observe a very slow decay component due to the effect of the photonic bandgap and an additional faster decay component probably due to QDs located in proximity to the etched holes of the photonic crystal. The extracted parameters are summarized in Tab. 1. We observe an enhancement in the total intensity of $\sim 4\times$ compared to the intensity of the QD ensemble in the bulk material, which we relate to a more efficient collection of the emitted photons due to angular redistribution of emission. [51, 30] If we take into account the air fill factor of 42 % of the photonic crystal structure, i.e. 42 % less QDs, the emission efficiency is even a factor $\sim 7\times$ higher than that observed from the bulk material.

Next, we focus on the waveguide region. Here, the oscillations in A_{fast} in Fig. 4 are an artifact of the slightly rotated waveguide structure and the $1 \mu\text{m}$ steps during the scan. We observe a highly enhanced amplitude for both the fast and slow decay components, as can be seen in the example transient in Fig. 4 marked by Ⓒ. The extracted parameters are summarized in Tab. 1. With a total intensity of 1116 ± 234 cts/s the PL signal detected from the PCW is a factor of $\sim 4\times$ stronger than on the PC membrane. This enhancement corresponds to the spatial influence of the waveguide mode. The higher photonic density of states in spatial and spectral resonance with the PCW mode reduces the radiative lifetime of the electron-hole pairs via the Purcell effect. [23] Since radiative and non-radiative recombination are competing processes in self-assembled QDs and typical non-radiative recombination rates are comparable to the radiative emission rates of QDs emitting into the photonic bandgap, [52] a reduction in the radiative lifetime will effectively increase the radiative quantum efficiency. As discussed above, the average lifetime of the QDs emitting into the photonic bandgap is lengthened to $\sim 4 - 5$ ns in our sample. This value is comparatively small when compared to literature where values of $\sim 10 - 12$ ns [34, 30] and up to ~ 20 ns [17, 21] have been reported. We attribute this difference to a distinct non-radiative recombination rate in this specific sample, possibly due to non-ideal growth or etching conditions. Together with a smaller effective air fill factor at the position of the PCW, the suppression

of non-radiative recombination due to Purcell enhanced radiative recombination can explain the increase in intensity detected from the waveguide region. Finally, compared to the emission from QDs in the bulk material, the measured intensity of 1116 ± 234 cts/s from the waveguide is a factor of $\sim 17\times$ higher in good agreement to the emission enhancement of $\sim 21\times$ extracted from Figs. 1 and 2. Furthermore, the measured lifetimes of 0.15 – 0.5 ns are slightly reduced compared to the lifetime of QDs in the bulk material of 0.5 – 0.6 ns, which leads to a moderate Purcell factor of 1 – 4.

In summary, we have demonstrated a $\sim 21\times$ higher out-of-plane emission intensity for quantum dots spectrally and spatially in resonance with the photonic crystal waveguide mode, as compared to quantum dots located in the unpatterned bulk material. By comparing the emission dynamics for the different photonic environments we could identify this emission enhancement as a combination of angular redistribution of emission and Purcell enhanced emission of quantum dot transitions into the waveguide mode and subsequent scattering into vertical directions. This broadband enhancement of the photoluminescence rate and intensity can be used for the construction of efficient light emitting diodes or single photon sources for optical computation applications.

Acknowledgements

We gratefully acknowledge financial support of the DFG via the SFB 631, the German Excellence Initiative via NIM, the EU-FP7 via SOLID, and the BMBF via QuaHLRep project 01BQ1036. AL acknowledges support of the TUM-GS, and SF of the Alexander von Humboldt Foundation.

References

- [1] S. Hughes. Coupled-cavity qed using planar photonic crystals. *Phys. Rev. Lett.*, 98:083603, 2007.
- [2] D. Englund, A. Faraon, B. Zhang, Y. Yamamoto, and J. Vučković. Generation and transfer of single photons on a photonic crystal chip. *Optics Express*, 15:5550, 2007.
- [3] Valentyn S. Volkov, Sergey I. Bozhevolnyi, Lars H. Frandsen, and Martin Kristensen. Direct observation of surface mode excitation and slow light coupling in photonic crystal waveguides. *Nano Letters*, 7:2341, 2007.
- [4] A. Faraon, I. Fushman, D. Englund, N. Stoltz, P. Petroff, and J. Vučković. Dipole induced transparency in waveguide coupled photonic crystal cavities. *Optics Express*, 16:12154, 2008.
- [5] Peijun Yao, V. S. C. Manga Rao, and S. Hughes. On-chip single photon sources using planar photonic crystals and single quantum dots. *Laser & Photonics Reviews*, 4:499, 2010.
- [6] P. Yao and S. Hughes. Controlled cavity qed and single-photon emission using a photonic-crystal waveguide cavity system. *Phys. Rev. B*, 80:165128, 2009.
- [7] Dirk Englund, Brendan Shields, Kelley Rivoire, Fariba Hatami, Jelena Vučković, Hongkun Park, and Mikhail D. Lukin. Deterministic coupling of a single nitrogen vacancy center to a photonic crystal cavity. *Nano Letters*, 10:3922, 2010.
- [8] Andre Schwagmann, Sokratis Kalliakos, Ian Farrer, Jonathan P. Griffiths, Geb A. C. Jones, David A. Ritchie, and Andrew J. Shields. On-chip single photon emission from an integrated

- semiconductor quantum dot into a photonic crystal waveguide. *Appl. Phys. Lett.*, 99(26):261108, 2011.
- [9] A. Laucht, S. Pütz, T. Günthner, N. Hauke, R. Saive, S. Frédérick, M. Bichler, M.-C. Amann, A. W. Holleitner, M. Kaniber, and J. J. Finley. A waveguide-coupled on-chip single-photon source. *Phys. Rev. X*, 2:011014, 2012.
- [10] S. Hughes. Enhanced single-photon emission from quantum dots in photonic crystal waveguides and nanocavities. *Opt. Lett.*, 29:2659, 2004.
- [11] E. Viasnoff-Schwoob, C. Weisbuch, H. Benisty, S. Olivier, S. Varoutsis, I. Robert-Philip, R. Houdré, and C. J. M. Smith. Spontaneous emission enhancement of quantum dots in a photonic crystal wire. *Phys. Rev. Lett.*, 95:183901, 2005.
- [12] G. Lecamp, P. Lalanne, and J. P. Hugonin. Very large spontaneous-emission beta factors in photonic-crystal waveguides. *Phys. Rev. Lett.*, 99:023902, 2007.
- [13] V. S. C. Manga Rao and S. Hughes. Single quantum-dot Purcell factor and beta factor in a photonic crystal waveguide. *Phys. Rev. B*, 75(20):205437, 2007.
- [14] V. S. C. Manga Rao and S. Hughes. Single quantum dot spontaneous emission in a finite-size photonic crystal waveguide: Proposal for an efficient “on chip” single photon gun. *Phys. Rev. Lett.*, 99(19):193901, 2007.
- [15] Wolfgang C. Stumpf, Masayuki Fujita, Makoto Yamaguchi, Takashi Asano, and Susumu Noda. Light-emission properties of quantum dots embedded in a photonic double-heterostructure nanocavity. *Appl. Phys. Lett.*, 90(23):231101, 2007.
- [16] V. S. C. Manga Rao and S. Hughes. Numerical study of exact purcell factors in finite-size planar photonic crystal waveguides. *Optics Letters*, 33(14):1587, 2008.
- [17] T. Lund-Hansen, S. Stobbe, B. Julsgaard, H. Thyrrestrup, T. Suenner, M. Kamp, A. Forchel, and P. Lodahl. Experimental realization of highly efficient broadband coupling of single quantum dots to a photonic crystal waveguide. *Phys. Rev. Lett.*, 101:113903, 2008.
- [18] M. Patterson, S. Hughes, D. Dalacu, and R. L. Williams. Broadband purcell factor enhancements in photonic-crystal ridge waveguides. *Phys. Rev. B*, 80:125307, 2009.
- [19] S. J. Dewhurst, D. Granados, D. J. P. Ellis, A. J. Bennett, R. B. Patel, I. Farrer, D. Anderson, G. A. C. Jones, D. A. Ritchie, and A. J. Shields. Slow-light-enhanced single quantum dot emission in a unidirectional photonic crystal waveguide. *Appl. Phys. Lett.*, 96:031109, 2010.
- [20] Luca Sapienza, Henri Thyrrestrup, Sren Stobbe, Pedro David Garcia, Stephan Smolka, and Peter Lodahl. Cavity quantum electrodynamics with anderson-localized modes. *Science*, 327(5971):1352, 2010.
- [21] Henri Thyrrestrup, Luca Sapienza, and Peter Lodahl. Extraction of the beta-factor for single quantum dots coupled to a photonic crystal waveguide. *Appl. Phys. Lett.*, 96:231106, 2010.
- [22] Thang Ba Hoang, Johannes Beetz, Leonardo Midolo, Matthias Skacel, Matthias Lerner, Martin Kamp, Sven Hofling, Laurent Balet, Nicolas Chauvin, and Andrea Fiore. Enhanced spontaneous emission from quantum dots in short photonic crystal waveguides. *Appl. Phys. Lett.*, 100(6):061122, 2012.
- [23] E. M. Purcell. Spontaneous emission probabilities at radio frequencies. *Phys. Rev.*, 69(1-2):681–681, 1946.
- [24] M Pelton, C Santori, J Vuckovic, BY Zhang, GS Solomon, J Plant, and Y Yamamoto. Efficient source of single photons: A single quantum dot in a micropost microcavity. *Phys. Rev. Lett.*, 89(23):233602, 2002.
- [25] C Santori, D Fattal, J Vuckovic, GS Solomon, and Y Yamamoto. Indistinguishable photons from a single-photon device. *Nature*, 419(6907):594, 2002.
- [26] Julien Claudon, Joel Bleuse, Nitin Singh Malik, Maela Bazin, Perine Jaffrennou, Niels Gregersen, Christophe Sauvan, Philippe Lalanne, and Jean-Michel Gerard. A highly efficient single-photon source based on a quantum dot in a photonic nanowire. *Nature Photonics*, 4:174, 2010.
- [27] Masazumi Fujiwara, Kiyota Toubaru, Tetsuya Noda, Hong-Quan Zhao, and Shigeki Takeuchi. Highly Efficient Coupling of Photons from Nanoemitters into Single-Mode Optical Fibers. *Nano*

- Letters*, 11(10):4362, 2011.
- [28] M. Davanco, M. T. Rakher, W. Wegscheider, D. Schuh, A. Badolato, and K. Srinivasan. Efficient quantum dot single photon extraction into an optical fiber using a nanophotonic directional coupler. *Appl. Phys. Lett.*, 99(12):121101, 2011.
- [29] Hatice Altug, Dirk Englund, and Jelena Vuckovic. Ultrafast photonic crystal nanocavity laser. *Nature Physics*, 2(7):484, 2006.
- [30] M. Kaniber, A. Laucht, T. Hürlimann, M. Bichler, R. Meyer, M.-C. Amann, and J. J. Finley. Highly efficient single-photon emission from single quantum dots within a two-dimensional photonic band-gap. *Phys. Rev. B*, 77:073312, 2008.
- [31] A. Kiraz, M. Atatüre, and A. Imamoglu. Quantum-dot single-photon sources: Prospects for applications in linear optics quantum-information processing. *Phys. Rev. A*, 69:032305, 2004.
- [32] W. H. Chang, W. Y. Chen, H. S. Chang, T. P. Hsieh, J. I. Chyi, and T. M. Hsu. Efficient single-photon sources based on low-density quantum dots in photonic-crystal nanocavities. *Phys. Rev. Lett.*, 96(11):117401, 2006.
- [33] D. Englund, D. Fattal, E. Waks, G. Solomon, B. Zhang, T. Nakaoka, Y. Arakawa, Y. Yamamoto, and J. Vučković. Controlling the spontaneous emission rate of single quantum dots in a two-dimensional photonic crystal. *Phys. Rev. Lett.*, 95(1):013904, 2005.
- [34] M. Kaniber, A. Kress, A. Laucht, M. Bichler, R. Meyer, M. C. Amann, and J. J. Finley. Efficient spatial redistribution of quantum dot spontaneous emission from two-dimensional photonic crystals. *Appl. Phys. Lett.*, 91(6):061106, 2007.
- [35] A. Laucht, F. Hofbauer, N. Hauke, J. Angele, S. Stobbe, M. Kaniber, G. Böhm, P. Lodahl, M.-C. Amann, and J. J. Finley. Electrical control of spontaneous emission and strong coupling for a single quantum dot. *New J. Phys.*, 11(2):023034, 2009.
- [36] D. Englund, A. Faraon, I. Fushman, N. Stoltz, P. Petroff, and J. Vučković. Controlling cavity reflectivity with a single quantum dot. *Nature*, 450(7171):857–861, 2007.
- [37] RSoft. Rsoft design group products. <http://www.rsoftdesign.com/>.
- [38] Steven G. Johnson, Pierre R. Villeneuve, Shanhui Fan, and J. D. Joannopoulos. Linear waveguides in photonic-crystal slabs. *Phys. Rev. B*, 62:8212, 2000.
- [39] D. F. Dorfner, T. Hürlimann, T. Zabel, L. H. Frandsen, G. Abstreiter, and J. J. Finley. Silicon photonic crystal nanostructures for refractive index sensing. *Appl. Phys. Lett.*, 93:181103, 2008.
- [40] K. Hennessy, A. Badolato, M. Winger, D. Gerace, M. Atatuerere, S. Gulde, S. Faelt, E. L. Hu, and A. Imamoglu. Quantum nature of a strongly coupled single quantum dot-cavity system. *Nature*, 445(7130):896, 2007.
- [41] A. Laucht, N. Hauke, J. M. Villas-Bôas, F. Hofbauer, G. Böhm, M. Kaniber, and J. J. Finley. Dephasing of exciton polaritons in photoexcited ingaas quantum dots in gaas nanocavities. *Phys. Rev. Lett.*, 103(8):087405, 2009.
- [42] F. Adler, M. Geiger, A. Bauknecht, F. Scholz, H. Schweizer, M. H. Pilkuhn, B. Ohnesorge, and A. Forchel. Optical transitions and carrier relaxation in self assembled InAs/GaAs quantum dots. *J. Appl. Phys.*, 80:4019, 1996.
- [43] A. Laucht, N. Hauke, A. Neumann, T. Guenther, F. Hofbauer, A. Mohtashami, K. Mueller, G. Boehm, M. Bichler, M. C. Amann, M. Kaniber, and J. J. Finley. Nonresonant feeding of photonic crystal nanocavity modes by quantum dots. *J. Appl. Phys.*, 109(10):102404, 2011.
- [44] P. W. Anderson. Absence of diffusion in certain random lattices. *Phys. Rev.*, 109:1492, Mar 1958.
- [45] Ad Lagendijk, Bart van Tiggelen, and Diederik S. Wiersma. Fifty years of anderson localization. *Physics Today*, 62(8):24, 2009.
- [46] S. R. Huisman, G. C. Stastis, S. Stobbe, A. P. Mosk, J. L. Herek, A. Lagendijk, P. Lodahl, W. L. Vos, and P. W. H. Pinkse. Photonic-Crystal Waveguides with Disorder: Measurement of a Band-Edge Tail in the Density of States. *arXiv:1201.0624*, January 2012.
- [47] E. Kuramochi, M. Notomi, S. Hughes, A. Shinya, T. Watanabe, and L. Ramunno. Disorder-induced scattering loss of line-defect waveguides in photonic crystal slabs. *Phys. Rev. B*, 72:161318, 2005.

- [48] M. Patterson, S. Hughes, S. Combrie, N. V. Quynh Tran, A. De Rossi, R. Gabet, and Y. Jaouen. Disorder-Induced Coherent Scattering in Slow-Light Photonic Crystal Waveguides. *Phys. Rev. Lett.*, 102:253903, 2009.
- [49] M. Patterson and S. Hughes. Theory of disorder-induced coherent scattering and light localization in slow-light photonic crystal waveguides. *J. Opt.*, 12:104013, 2010.
- [50] D. P. Fussell, S. Hughes, and M. M. Dignam. Influence of fabrication disorder on the optical properties of coupled-cavity photonic crystal waveguides. *Phys. Rev. B*, 78:144201, 2008.
- [51] M Fujita, S Takahashi, Y Tanaka, T Asano, and S Noda. Simultaneous inhibition and redistribution of spontaneous light emission in photonic crystals. *Science*, 308:1296, 2005.
- [52] Jeppe Johansen, Søren Stobbe, Ivan S. Nikolaev, Toke Lund-Hansen, Philip T. Kristensen, Jørn M. Hvam, Willem L. Vos, and Peter Lodahl. Size dependence of the wavefunction of self-assembled inas quantum dots from time-resolved optical measurements. *Phys. Rev. B*, 77:073303, 2008.